Received May 14, 2019, accepted May 28, 2019, date of publication June 27, 2019, date of current version July 18, 2019.

Digital Object Identifier 10.1109/ACCESS.2019.2925466

Formation Control of Multiple Unmanned Surface Vehicles Using the Adaptive Null-Space-Based Behavioral Method

JIAJIA FAN, YULEI LIAO, YE LI, QUANQUAN JIANG, LEIFENG WANG, AND WEN JIANG
Science and Technology on Underwater Vehicle Laboratory, Harbin Engineering University, Harbin 150001, China

Corresponding author: Yulei Liao (liaoyulei@hrbeu.edu.cn)

This work was supported in part by the National Key Research and Development Program of China under Grant 2017YFC0305700, in part by the National Natural Science Foundation of China under Grant 51779052, Grant U1806228, and Grant 51879057, in part by the Research Fund from the Science and Technology on Underwater Vehicle Laboratory under Grant 614221503091701, in part by the Fundamental Research Funds for the Central Universities under Grant HEUCFG201810, and in part by the Qingdao National Laboratory for Marine Science and Technology under Grant QNLM2016ORP0406.

ABSTRACT This paper presents an adaptive null-space-based behavioral (NSB) method to deal with the problems of saturation planning and lack of adaptability when the traditional NSB method is applied to the formation control of multiple unmanned surface vehicles (MUSVs). First, the NSB method is analyzed, and the matrix theory is introduced to propose a behavior priority theory determination method based on a vector graph. Second, consider the maneuverability of the unmanned surface vehicle (USV), variable coefficients with physical significances are introduced to redefine the behavioral motion model, making the speed limit solved in each working condition within the maneuvering range of the USV and effectively improving the formation ability of MUSVs. Third, a logical priority collision avoidance strategy between the MUSVs is proposed, aiming at the problem that when the USVs judge each other as obstacles, both of them adopt the obstacle avoidance behavior resulting in two vehicles' courses deviating from the direction of the target point. Finally, a simulation platform for the formation control of MUSVs was established by taking the Dolphin-I prototype USV as the experimental object, and the feasibility of the proposed method was verified by a simulation test.

INDEX TERMS Multiple unmanned surface vehicles (MUSVs), adaptability formation control, null-space-based behavior (NSB), behavior priority, cooperative collision avoidance.

I. INTRODUCTION

The unmanned surface vehicle (USV), an underactuated vehicle, is used for dangerous and inhospitable missions [1], [2]. The multiple unmanned surface vehicles (MUSVs) system [3]–[6] has attracted increasing attention due to its low cost, and robustness. In recent years, the coordination of MUSVs has become a new research hotspot. Formation control of unmanned surface vehicles [7], [8] refers to the control technology in which multiple robots maintain a certain formation during transit to a destination while at the same time adapting to environmental constraints (such as the presence of obstacles and space constraints). Formation control of MUSVs is a typical and universal coordination problem. It is also the most important problem facing MUSVs system and is worth deep and detailed investigation.

To solve the MUSVs formation problem, centralized [9], [10] distributed [11], [12] formation control methods are often adopted. Compared with the centralized method, the distributed method has become a hotspot in unmanned surface vehicle formation research because of its high reliability, and good flexibility. The null-space-based behavior control (NSB) method is a typical method to study the distributed formation control problem [13]. In [11] and [12], the NSB method was applied to the formation control of underactuated unmanned surface vehicles to simulate formation navigation tasks under sea currents and faced with obstacles. In [14], the formation control method was adopted based on the NSB method and applied to the distributed multi-soccer robots, transforming the environment

The associate editor coordinating the review of this manuscript and approving it for publication was Sara Dadras.

from two-dimensional space to three-dimensional space. The NSB method was also applied to the collaborative control of spacecraft formation to solve problems such as global movement, global convergence and dispersion, configuration transformation, and collision avoidance [15]. In [16] and [17], research tackled the problem of precise formation control of the multi-Euler Lagrange system with model uncertainty in the obstacle environment; the gain of the obstacle avoidance task was determined by using sliding-mode control and Lyapunov theory in NSB obstacle avoidance behavior.

The above methods are based on the traditional NSB method for formation control. In application, since the gain coefficients of this method are constant coefficients (without clear physical significance) and are constrained by robot motion factors (velocity, starting point, and ending point), their values need to be reselected and debugged under each working condition. This lacks adaptability and is not conducive to engineering applications. Moreover, because the gain coefficients are constant at each fixed condition, the traditional NSB formation control method will produce the saturated planning phenomenon; the planned expected speed is higher than the actual speed limit of the robot (exceeding its maneuverability) and task failure will occur. At the same time, the traditional NSB method does not have a theoretical definition of behavior priority and is mostly based on empirical sorting.

In this paper, the traditional NSB method is first analyzed, and a vector analysis method based on a vector graph to determine the behavior priority is proposed. Second, combined with the maneuverability of the USV, an adaptive null-space-based behavioral (ANSB) control method is put forward. By introducing the variable coefficients with physical significance to redefine the behavioral motion model, the speed limit calculated in each working condition is within the maneuverability range of USV. Third, aiming at the problem when the USVs judge each other as obstacles, both of them adopt the obstacle avoidance behavior resulting in two vehicles' courses deviating from the direction of the target point, a logical priority collision avoidance strategy between the MUSVs is proposed. Finally, a simulation platform for formation control of multiple unmanned surface vehicles was established by using the Dolphin-I prototype USV as the experimental object; simulation results demonstrated that the ANSB method can effectively improve the formation performance of MUSVs.

II. ANALYSIS AND DESIGN OF THE USV GUIDANCE SYSTEM

MUSVs control system includes a navigation subsystem, guidance subsystem, and motion control subsystem [18]. The guidance subsystem deals with navigation; a feasible navigation path can be continuously generated according to the navigation system's information, task requirements, and environmental status, and the reference path can then be sent to the control subsystem [19]. The distributed NSB formation control method undertakes the tasks of path planning and trajectory tracking in the centralized formation control method, and forms the guidance system of the USV.

This paper first briefly analyzes the theory of the NSB method, and then proposes a theoretical determination method of behavior priority based on a vector graph combined with the matrix method [20]. Finally, a dynamic model of the Dolphin series mini-type MUSVs is described.

A. NULL-SPACE-BASED BEHAVIORAL THEORY

The null-space-based behavioral method is a typical distributed control formation method [21]. The central idea is to decompose the task into different behaviors, such as target reaching, collision avoidance, and cooperative formation, and use the matrix theory method of null space to fuse the behaviors according to a certain priority.

We assume that x and y are the coordinates under the inertial coordinate system, and set the coordinate position of USV as $p_i = [x_i, \mathrm{y}_i]^T$, the linear velocity of navigation as $v_i = [\dot{x}_i, \dot{\mathrm{y}}_i]^T$, the position of the target point as $p_t = [x_t, y_t]^T$, the obstacle coordinate as $p_a = [x_a, y_a]^T$, and σ as the task function in the behavior control:

$$\sigma = f(p) \tag{1}$$

We take the derivative of both sides of equation (1):

$$\dot{\sigma} = \frac{\partial f(p)}{\partial p} v = J(p)v \tag{2}$$

where $J(p)$ is the Jacobian matrix of σ. Then, the expected velocity of the USV is

$$v = J^{\dagger}\dot{\sigma} \tag{3}$$

where v is the expected speed for a single behavior, and $J^{\dagger}$ is the generalized inverse matrix of J. If the system needs to execute multiple behaviors $\sigma_1, \sigma_2, \sigma_3 \ldots$ at the same time, the priority of each behavior is specified and the subscript is used to indicate the expected speed of multiple behaviors, such as $v_1, v_2, v_3 \ldots$. Then, the NSB method can be used to fuse multiple behaviors and obtain the final velocity as follows:

$$v = v_j + (I - J_j^{\dagger} J_j) v_{j+1} \tag{4}$$

where $\mathrm{Null}(j) = I - J_j^{\dagger} J_j$ is the null space of the task velocity matrix of level j.

B. VECTOR GRAPH BEHAVIOR PRIORITY DETERMINATION METHOD

Definition 1: Given that A is a matrix, the null-space of A, also known as the kernel, is a set of n-dimensional vectors [20]:

$$\mathrm{Null}(A) = \{x \in R^n : Ax = 0\} \tag{5}$$

The null-space-based behavioral method projects the level $i+1$ task vector to the level i task vector and obtains the new task output, that is, when the system completes a high-priority behavior, it maps a low-priority behavior to the output matrix

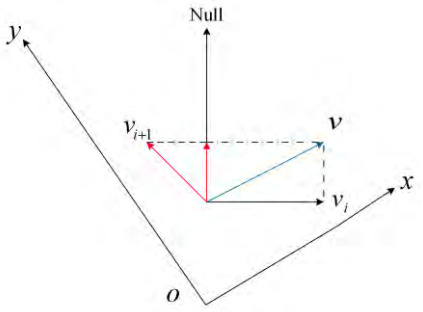

FIGURE 1. Schematic diagram of null-space-based behavior mapping.

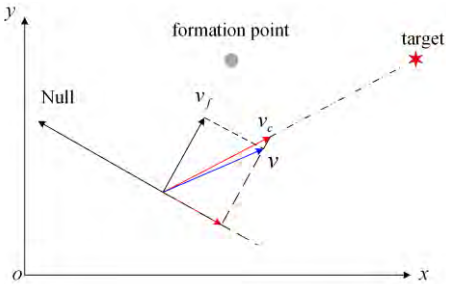

FIGURE 2. Vector graph of the cooperative formation behavior with a higher priority than the target reaching behavior.

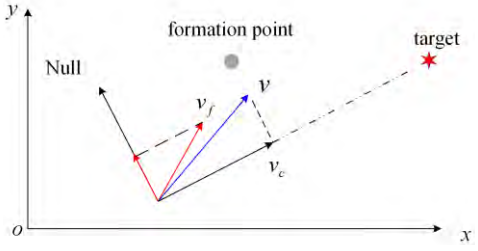

FIGURE 3. Vector graph of the target reaching behavior with a higher priority than the cooperative formation behavior.

of the high-priority behavior so as to complete some low-priority behavior [11], [21]. Fig.1 shows a schematic diagram of the behavior mapping.

Based on behavior mapping, we propose a method to determine the behavior priority namely vector graph analysis of the NSB formation control method. Two indistinguishable behaviors (cooperative formation and target reaching) are taken as examples, and the schematic diagrams for these behaviors are shown in Fig.2 and Fig.3.

The velocities of the cooperative formation behavior and target reaching behavior are represented by v_f and v_c, respectively. When prioritizing two behaviors, there are two combinations: the first combination is that the priority of cooperative formation behavior is higher than that of the target reaching behavior, and the second combination is that the target reaching behavior is of a higher priority than the cooperative formation behavior. The fusion velocity results of the two combinations using the vector graph determination method are shown in Fig.2 and Fig.3. In Fig.2, v_c is projected

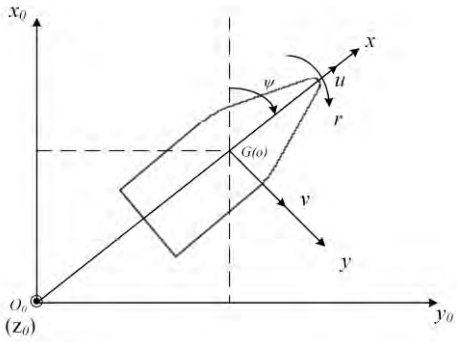

FIGURE 4. Unmanned surface vehicle coordinate system.

to the null space of v_f, and is fused with the velocity v_f at high priority. In Fig.3, v_f is projected to the null space of v_c, and is fused with the velocity v_c at high priority. Compared with the first combination, the fusion velocity in the second combination was more oriented to the desired formation point, which was conducive to accelerating formation.

The behavior priority based on the vector graph determination method can theoretically rank the fusion of behaviors.

C. DYNAMIC MODEL OF USV

In this paper, the formation system of the Dolphin series mini-type MUSVs is established. In order to describe the motion of an USV, two right-handed rectangular coordinate systems are adopted [22]. The first coordinate system is the inertial frame $o_0 - x_0y_0z_0$ and the second is the body-coordinate system $o - xy$ (Fig.4). The inertial frame is fixed on the earth. The plane $o_0 - x_0y_0$ is on the undisturbed free surface and the x_0 axis points toward the initial straight course of the USV with the z_0 axis going straight down. The body-coordinate system is fixed on the vehicle and the origin is located in the middle of the vehicle. The plane $o - xy$ is on the undisturbed free surface. The x axis points to the bow, the y axis points starboard, and the z axis points straight down.

Since the transverse speed can be neglected without considering the external environment interference, the maneuverability model of USV is as follows:

$$\begin{cases} \dot{x} = u\cos\psi \\ \dot{y} = u\sin\psi \\ \dot{\psi} = r \\ \dot{r} = \dfrac{1}{T}(K\delta - r - \alpha r^3) \\ u = k_1 n^2 + k_2 n + k_3 \end{cases} \tag{6}$$

where (x, y) is the position of the USV, u is the longitudinal speed, ψ is the heading angle, r is the heading angular velocity, δ is the rudder angle, and K, T, and α are the motion model parameters. Dolphin-I is a mini unmanned catamaran. Referring to the model of thrust and velocity in reference [23], the corresponding relationship between the speed and voltage of the USV was established. n is the propeller's voltage, and k_1, k_2, k_3 are propulsion system parameters. The main parameters of the Dolphin-I USV are shown in Table 1.

TABLE 1. Main parameters of Dolphin-I.

Parameters	Parameter values
Length	2.0 m
Spacing between two floating body	1.1 m
Maximum speed	1.2 m/s
Propulsion method	Two propellers with a rear-mounted rudder plate
Maneuverability model	$K=0.287,\ T=0.410,\ \alpha=0.009$
Velocity model	$k_1=-0.006,\ k_2=0.159,\ k_3=0.004$

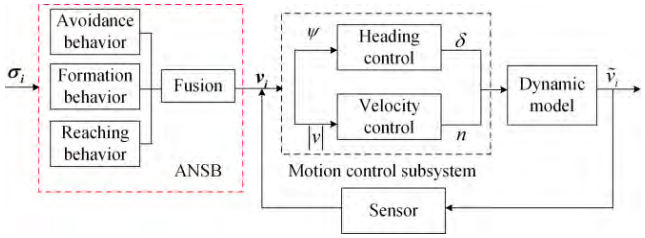

FIGURE 5. Principle block diagram of the USV control system.

To sum up, the principle of the USV control system adopting the null-space-based behavioral formation control method is shown in Fig.5.

In Fig.5, σ_i contains σ_{ic}, σ_{ia}, and σ_{if}, which respectively represent the task functions of three behaviors of the i-th USV. $v_i(v_x, v_y)$ is the expected velocity vector calculated by the NSB method, and $\widetilde{v}_i$ is the actual velocity vector of the USV. ψ and $|v|$ are the inputs of the motion control subsystem and propulsion control subsystem, respectively. δ and n are the corresponding outputs of the two systems. The expected heading angle of the USV can be obtained by Eq.7.

$$\psi = \begin{cases} \arctan\left(\dfrac{v_y}{v_x}\right) & v_x \geq 0 \\ \arctan\left(\dfrac{v_y}{v_x}\right) + \pi & v_x < 0, v_y \geq 0 \\ \arctan\left(\dfrac{v_y}{v_x}\right) - \pi & v_x < 0, v_y < 0 \end{cases} \tag{7}$$

III. ADAPTIVE NULL-SPACE-BASED BEHAVIORAL METHOD

In application, since the gain coefficients of the traditional NSB method are constant coefficients (without clear physical significance) and are constrained by robot motion factors (velocity, starting point, and ending point), their values need to be reselected and debugged under each working condition. This lacks adaptability and is not conducive to engineering applications. The adaptive null-space-based behavioral method redefines the behavioral motion model by introducing the variable coefficient with physical significance (the maximum speed of USV, the terminal coordinate, and the current positioning coordinate). Therefore, the speed limit calculated in each working condition is within the maneuverability range of the USV. Compared with the traditional NSB method, the ANSB method is adaptive and can consider both the efficiency and the maneuverability of the USV.

We set the coordinate position of the USV as $p_i = [x_i, y_i]^T$, the linear velocity of navigation as $v_i = [\dot{x}_i, \dot{y}_i]^T$, the position of the target point as $p_t = [x_t, y_t]^T$, the obstacle coordinate as $p_a = [x_a, y_a]^T$, the task function in the behavior control as σ, the expected value of the behavior control variable as σ_d, and the gain coefficient as λ. In the traditional NSB control method, (3) can be changed to obtain (8).

$$v_i = J_i^{\dagger}\lambda_i(\sigma_d - \sigma) \tag{8}$$

According to the requirements of USV operation, task execution is divided into three behaviors: target reaching behavior, collision avoidance behavior, and cooperative formation behavior. According to the physical meaning of each behavior, the behavior gain coefficient of the ANSB method is redefined to make the method have the speed controllability and the working condition adaptability.

A. MATHEMATICAL MODEL OF TARGET REACHING BEHAVIOR

The target reaching behavior runs throughout the MUSVs' operation. The mathematical model of this behavior is shown in (9)–(11). By introducing the maximum speed, real-time coordinate position, and terminal position of the USV, the gain coefficient of the target reaching behavior is redefined to ensure that the final speed calculated is always within the maneuverability range of the USV and thus we effectively avoid the phenomenon of "saturation planning".

$$v_c = J_c^{+}(p)\lambda_c(p_t - p_i) \tag{9}$$

$$\lambda_c = v_{\max} \cdot \frac{1}{\sqrt{D_c^2 + r_c^2}} \tag{10}$$

$$D_c = \sqrt{(x_t - x_i)^2 + (y_t - y_i)^2} \tag{11}$$

where the variable $r_c > 0$ is the regulatory factor of the target reaching behavior.

As shown in (10), after redefining the gain coefficient λ_c, the expected speed of the target trend behavior is less than the maximum speed, that is, $|v_c| < v_{\max}$. r_c is introduced to solve the phenomenon where the USV does not reach the target point with the traditional NSB method and the sudden and uncontrollable large deceleration leads to slow speed and a slow change in the expected path point.

B. MATHEMATICAL MODEL OF COLLISION AVOIDANCE BEHAVIOR

In the course of MUSVs navigation, collision avoidance behavior can guarantee the safety of MUSVs and provide a basic guarantee for the realization of subsequent tasks. The safe distance for collision avoidance is defined as d, D_a represents the distance between the USV and the obstacle, and λ_a represents the gain coefficient of collision avoidance behavior. The mathematical model of collision avoidance behavior is shown in (12)–(14).

$$v_a = J_a^{+}(p)\lambda_a(d - D_a) \tag{12}$$

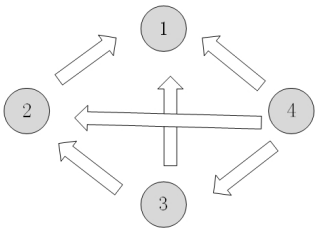

FIGURE 6. Schematic diagram of logical priority collision avoidance strategies between USVs.

$$\lambda_a = v_{\max} \cdot \frac{1}{(d - D_{a0})} J_{a0}(p) \tag{13}$$

$$D_a = \sqrt{(x_a - x_i)^2 + (y_a - y_i)^2} \tag{14}$$

where D_{a0}, J_{a0} are the values obtained by D_a, J_a at the initial moment of obstacle avoidance, and $D_{a0} < d$.

According to (12), the expected speed for the danger avoidance behavior of the USV is less than the maximum speed, that is, $|v_a| < v_{\max}$. When the USV is gradually approaching the obstacle, the expected speed decreases gradually. When it is infinitely close to the safe distance for obstacle avoidance, the expected speed of collision avoidance behavior is zero, and since the collision avoidance behavior is the highest-level behavior, the expected speed of the USV is zero.

When considering the problem of collision avoidance between MUSVs, a logical priority strategy is proposed; all the MUSVs in the formation should be numbered and an USV sees vehicles which numbered numbers are smaller as obstacles. This kind of collision avoidance strategy can effectively solve the problem when the USVs judge each other as obstacles, both of them adopt the obstacle avoidance behavior resulting in two vehicles' courses deviating from the direction of the target point. Fig.6 shows a schematic diagram of logical priority collision avoidance strategies between MUSVs.

C. MATHEMATICAL MODEL OF COOPERATIVE FORMATION BEHAVIOR

The formation of MUSVs is a complex task that involves cooperation between different MUSVs. In order to realize formation, a behavioral control function was established based on the distance deviation between the formation's form and the formation's center. The mathematical model of cooperative formation behavior is shown in (15)–(17).

$$v_f = J_f^+(p)\lambda_f(\delta_f - \delta_{f,d}) \tag{15}$$

$$\lambda_f = v_{\max} \cdot \frac{1}{\sqrt{D_f^2 + r_f^2}} \tag{16}$$

$$D_f = \sqrt{(x_f - x_i)^2 + (y_f - y_i)^2} \tag{17}$$

where δ_f is the actual horizontal and vertical coordinate deviation between the robot's current position point and the formation's center, and $\delta_{f,d}$ is the expected horizontal and vertical coordinate deviation between the robot's current position point and the formation's center. (x_f, y_f) is the desired formation position point of the USV at the current moment, and $r_f > 0$ is the formation threshold. In this behavior, it is considered that the formation and maintenance of the formation are interdependent, and that cooperative formation behavior is always accompanied by target reaching behavior so that robustness can increase during operation. Based on the vector graph method for determining behavior priority, it can be seen that the priority of the target reaching behavior is higher than that of the cooperative formation behavior, which is conducive to accelerating formation and maintenance of the formation. Therefore, when the cooperative formation behavior projects to the null space of the target reaching behavior, the fused velocity $|v_{cf}|$ is less than $v_{\max}$.

IV. NUMERICAL SIMULATION OF MUSVs FORMATION TEST

Taking the Dolphin-I prototype USV as the experimental object, the formation simulation platform of five unmanned surface vehicles was established to verify the adaptive null-space-based behavior formation control method proposed in this paper. The simulation platform was built using MATLAB software, and the PID control method [24] was adopted to control the course and speed.

A. COMPARATIVE EXPERIMENTS USING THE FORMATION CONTROL METHOD

The initial positions of the five USVs were $p_1 = (1\text{ m}, -10\text{ m})$, $p_2 = (6\text{ m}, -20\text{ m})$, $p_3 = (4\text{ m}, 20\text{ m})$, $p_4 = (8\text{ m}, 10\text{ m})$, and $p_5 = (10\text{ m}, 1\text{ m})$, respectively. The target position was (800 m, 100 m), the obstacle position was (300 m, 10 m), the obstacle radius was $r = 20$m, the influence radius was $r_{in} = 0.2 \times r$, and the iteration step length was 1 s. We suppose that the maximum speed of the USV was 1.5 m/s. The traditional NSB method adopted the same obstacle avoidance strategy and behavior priority as the ANSB method. The formation of MUSVs was expected to be a regular pentagonal shape, in which USV no.1 served as the vertex of the formation's forward direction. After several simulation tests, it was finally determined that when the gain coefficient of the three behaviors were $\lambda_c = 0.001, \lambda_f = 0.020$, and $\lambda_a = 0.025$, the expected speed calculated by the traditional NSB formation method would always remain within the maximum maneuvering speed range of the USV. The simulation results are shown in Fig. 7 and Fig. 8.

Fig.7 shows the path planning diagram of five USVs by the NSB method, and the dotted black line indicates the formation at every 200 iterations. Fig.8 shows the expected speed curve of USV no. 1 under the current mission condition; the red dotted line is the maximum maneuvering speed of the USV, and the blue solid line is the expected speed. It can be seen from Fig. 8 that when adopting the traditional NSB formation control method, the selected behavioral gain coefficient can make the maximum expected speed be calculated within the maneuvering range of the USV. However, the expected speed decreased exponentially. The expected

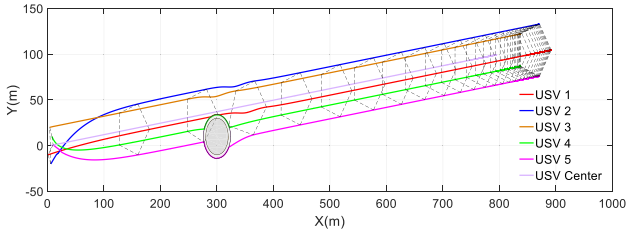

FIGURE 7. Planning path diagram of NSB (condition 1).

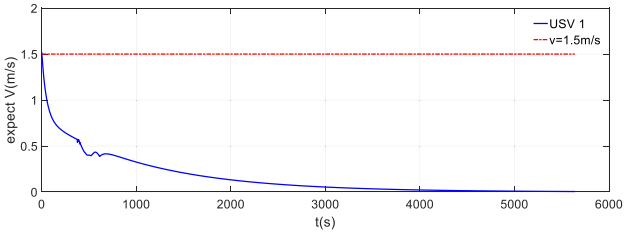

FIGURE 8. Expected speed of USV no.1 determined by NSB.

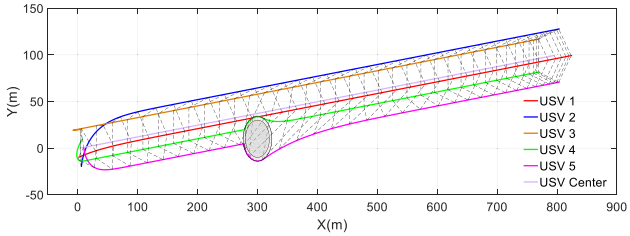

FIGURE 9. Planning path diagram of ANSB (condition 1).

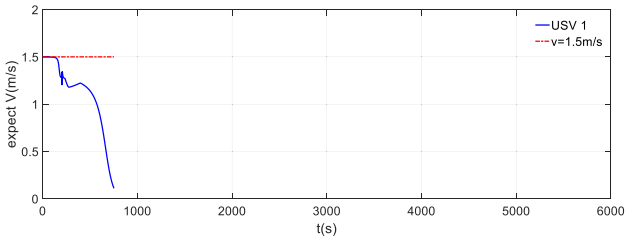

FIGURE 10. Expected speed of USV no.1 determined by ANSB.

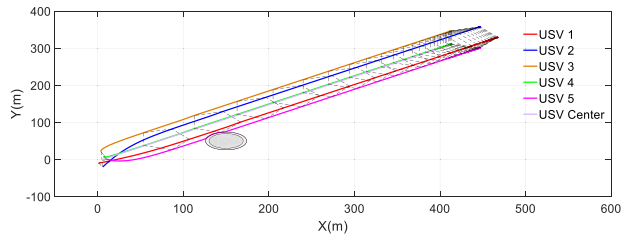

FIGURE 11. Planning path diagram of NSB (condition 2).

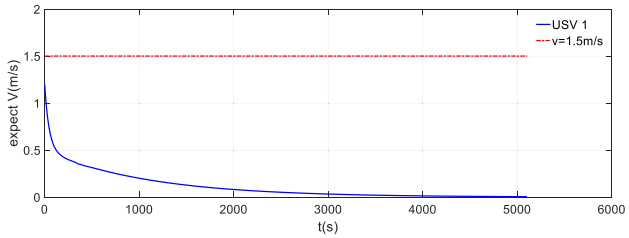

FIGURE 12. Expected speed of USV no.1 determined by NSB.

speed of the first third of the voyage was reduced to 0.2 m/s, resulting in a slow update of the position of the USV in the second half of the voyage. When encountering obstacles, the speed was adjusted to maintain formation.

Fig.9 and Fig.10 are USV paths under the same working condition using the ANSB formation control method. As shown in Fig. 7 and Fig.9, the priority collision avoidance strategy can effectively avoid that both vehicles perform the collision avoidance behavior against each other, and improve formation efficiency. The dotted black line in Fig. 9 shows the formation of MUSVs at every 20 iterations. Fig.10 shows the expected speed curve under the current task condition. As can be seen from Fig. 10, the expected speed of the USV always remained within the maximum maneuvering speed range, and slowly declined. When two-thirds of the distance was covered, the speed showed an obvious downward trend. When encountering obstacles, the speed was adjusted to maintain formation.

It can be seen from comparing Fig.8 and Fig.10 that under the current working condition, the navigation time of the ANSB method was reduced from 5,000 s by the traditional NSB method to less than 1,000 s. Therefore, the ANSB method can control the speed, optimize the speed change trend, and effectively improve the task completion rate.

B. COMPARATIVE EXPERIMENTS ON THE SHORT-DISTANCE FORMATION TASK

Under the same simulation environment, we control the iteration step size and behavioral gain coefficient by the traditional NSB method as in the above experiment. The formation of MUSVs sailed from the same position to a closer target point (400 m, 300 m) than the previous experiment. The obstacle position was (150 m, 50 m), the obstacle radius was $r = 20$m, and the influence radius was $r_{in} = 0.2 \times r$. The test results of two formation control methods are shown in Figs. 11–14.

According to Fig.12, with the same behavior gain coefficient, the maximum speed calculated by the traditional NSB method was only 3/4 of the maximum maneuver speed at the early stage of planning, and then the speed decreased exponentially. At 300 iterations, the expected speed dropped to 0.3 m/s, and the number of iterations to complete tasks and reach the target point was more than 5,000.

Fig.14 shows the expected speed under the ANSB method. It can be seen from the figure that the expected speed was always within the maximum maneuvering range of the USV, and the speed trend was relatively gentle. When approaching the target point, the speed decreased slowly, and the number of iterations in the whole journey was approximately 500. Table 2 shows the detailed simulation results and the

TABLE 2. Detailed results for short-distance formation task performed by TWO methods.

NSB METHOD				ANSB METHOD			
Time (s)	Expected v (m/s)	Position X	Position Y	Time (s)	Expected v (m/s)	Position X	Position Y
2	1.19	2.09	-9.50	2	1.50	2.44	-9.58
202	0.42	107.33	54.72	22	1.50	30.03	2.05
602	0.29	217.30	139.21	62	1.50	80.31	34.61
1002	0.20	294.40	197.85	102	1.49	128.23	70.50
1402	0.14	348.19	238.76	142	1.28	174.46	105.65
1802	0.10	385.71	267.29	182	1.20	213.13	135.06
2202	0.07	411.88	287.20	222	1.17	250.76	163.68
2602	0.05	430.14	301.08	262	1.12	287.21	191.40
3002	0.03	442.87	310.77	302	1.05	321.95	217.82
3402	0.02	451.76	317.52	342	0.95	354.04	242.23
3802	0.02	457.95	322.24	382	0.79	381.95	263.45
4202	0.01	462.28	325.52	422	0.56	403.54	279.88
4602	0.01	465.29	327.82	462	0.31	417.38	290.40
5002	0.01	467.39	329.42	502	0.15	424.57	295.87

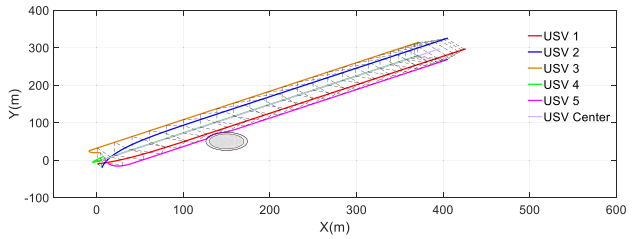

FIGURE 13. Planning path diagram of ANSB (condition 2).

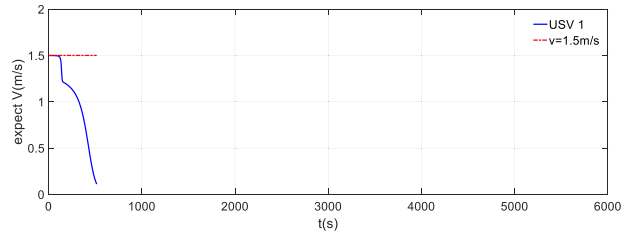

FIGURE 14. Expected speed of USV no.1 determined by ANSB.

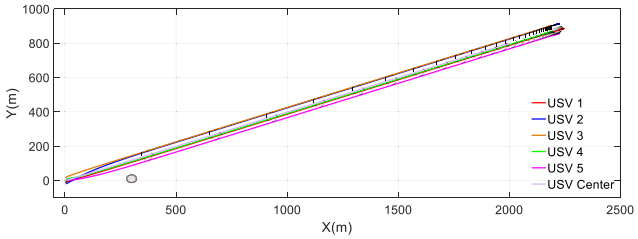

FIGURE 15. Planning path diagram of NSB (condition 3).

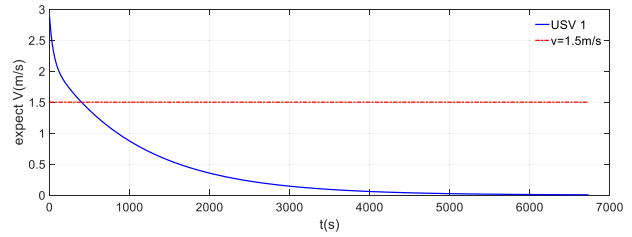

FIGURE 16. Expected speed of USV no.1 determined by NSB.

relationships between the expected speed, position coordinate, and number of iterations under the two methods.

C. COMPARATIVE EXPERIMENTS ON THE LONG-DISTANCE FORMATION TASK

Under the same simulation environment, we control the iteration step size and behavioral gain coefficient by the traditional NSB method as in the above experiment. In this task, the formation of MUSVs sailed from the same position to a distant target point (2000 m, 800 m). The test results of two formation control methods are shown in Figs. 15–18. The formation track of USVs under the two formation control methods is shown in Fig. 15 and Fig. 17. The dotted black line in Fig. 15 shows the formation of MUSVs at every 200 iterations, and the dotted black line in Fig. 17 represents the formation of MUSVs at every 20 iterations. According to the figures, both the traditional

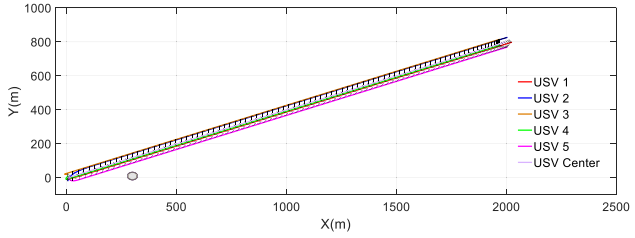

FIGURE 17. Planning path diagram of ANSB (condition 3).

NSB and the ANSB method can successfully complete the tasks. In Fig. 15, the trajectory update of the MUSVs became more and more slow after half the journey towards the target point. Meanwhile, in Fig. 17, the trajectories throughout the journey were relatively stable, and the trajectory update did not become slow until they approached the target point.

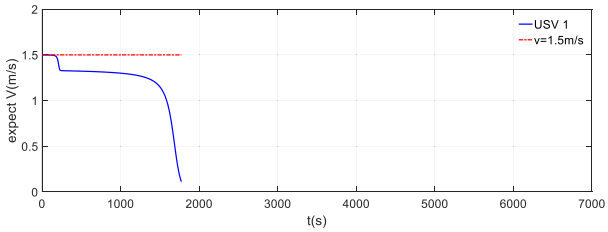

FIGURE 18. Expected speed of USV no.1 determined by ANSB.

TABLE 3. Comparison of two formation control methods.

Condition	Target (m)	NSB		ANSB	
		Maximum expected speed (m/s)	Sailing time (s)	Maximum expected speed (m/s)	Sailing time (s)
1	(800,100)	1.51	5602	1.50	742
2	(400,300)	1.19	5002	1.50	502
3	(2000,800)	2.85	6602	1.50	1762

Fig.16 reveals the expected speed under the NSB method. It can be seen from the figure that the expected speed in the first 400 iterations was significantly higher than the maximum maneuvering speed of the USV, resulting in saturation planning. In the subsequent planning, the speed was within the range of the maneuvering speed of the USV, but it decreased exponentially. At 2000 iterations, the expected speed decreased to 0.3 m/s, and the iteration step size under the current working condition for MUSVs to complete the task was more than 6000 s.

Fig.18 reveals the expected speed under the ANSB method. It can be seen from the figure that the expected speed was always within the maximum maneuvering range of the USV, and the speed trend was relatively gentle. When approaching the target point, the speed decreased slowly, and the number of iterations in the whole journey was less than 1800 s.

Table 3 illustrates that the ANSB formation control method in the long-distance task can achieve consistent with the first two test operation conditions, and can maximize the use of the USV's maneuverability. The ANSB method can effectively solve the problems of saturated planning and lengthy planning that plague the traditional NSB formation control method, thus improving efficiency on the formation task.

D. SIMULATION TEST OF THE ANSB METHOD UNDER THE NOMINAL MODEL

The MUSVs formation motion model was built on a simulation platform. This paper focused on the formation control of MUSVs, thus this platform adopted the classic PID control method to control course and speed of the single vehicle. The control law is shown in Eq. (18) [25]–[29].

$$w = K_p e + K_i \int e dt + K_d \frac{de}{dt} \tag{18}$$

where w is the output of the controller, and e is the deviation between the given expected value and actual output value.

FIGURE 19. The Dolphin-I developed by Harbin Engineering University.

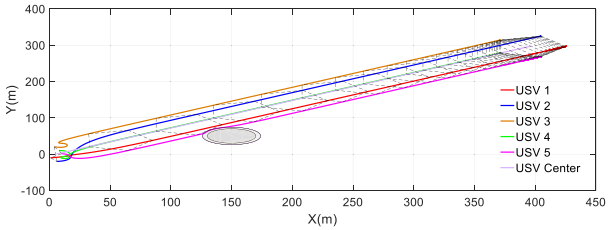

FIGURE 20. The track of MUSVs formation by the NSB method with a 2 m safe distance between USVs. (The gain coefficients of the three behaviors were $\lambda_c = 0.001$, $\lambda_f = 0.020$, and $\lambda_a = 0.025$).

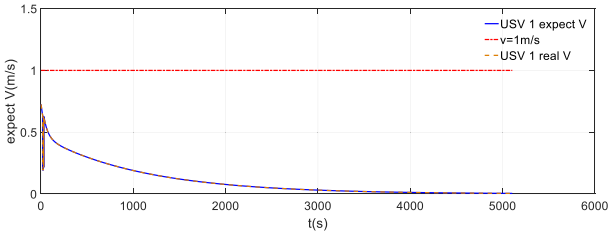

FIGURE 21. Speed contrast curve of USV no.1 determined by the NSB method.

The iterative step length and control cycle were both 0.1 s. The parameters of the course PID controller were set as $K_p = 1.0$, $K_i = 0.001$, and $K_d = 1.0$. The parameters of the speed controller were $K_p = 2.0$, $K_i = 0.001$, and $K_d = 0.001$. The dynamics model motion parameters for the Dolphin-I mini-type USV were $K = 0.287$, $T = 0.410$, and $\alpha = 0.009$, and the velocity model parameters were $k_1 = -0.006$, $k_2 = 0.159$, and $k_3 = 0.004$. Fig.19 shows a photo of Dolphin-I in the Songhua River.

The MUSVs formation operated under the same working conditions as in the above tests, but from the same starting point to a closer target point (400 m, 300 m). The obstacle position was (150 m, 50 m), the obstacle radius was $r = 20$m, and the influence radius was $r_{in} = 0.2 \times r$.

In the first group of comparative tests, the safe distance which was the minimum distance between two USVs to ensure safe navigation was set as 2 m. Fig. 20 and Fig. 21 show the simulation test results of five USVs in a cooperative formation task under the nominal model controlled by the traditional NSB method without a collision avoidance strategy.

The dotted black line in Fig.20 is the formation of the MUSVs every 200 s under the NSB method. As can be

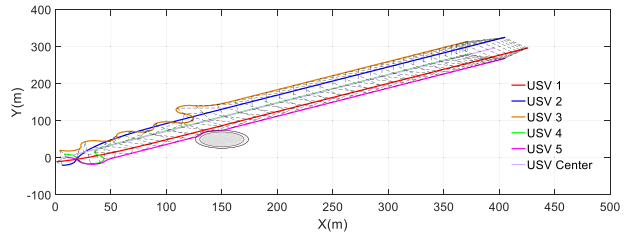

FIGURE 22. The track of MUSVs formation determined by the ANSB method with a 2 m safe distance between USVs.

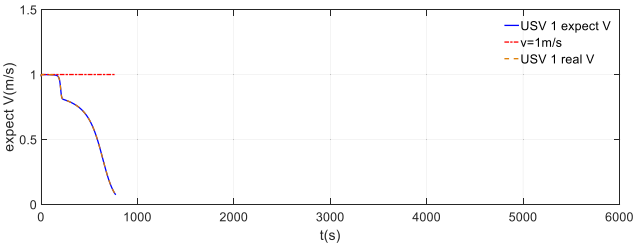

FIGURE 23. The speed contrast curve of USV no.1 determined by ANSB.

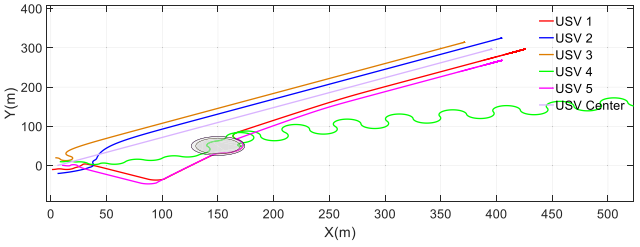

FIGURE 24. The track of USVs formation determined by the NSB method with a 10 m safe distance between USVs. (The gain coefficients of the three behaviors were $\lambda_c = 0.001$, $\lambda_f = 0.020$, and $\lambda_a = 0.025$).

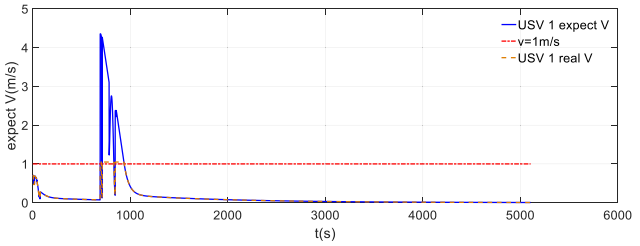

FIGURE 25. The speed contrast curve of USV no.1 determined by the NSB method.

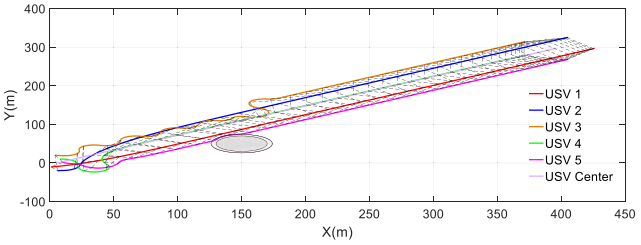

FIGURE 26. The track of MUSVs formation determined by the ANSB method with a 10 m safe distance between USVs.

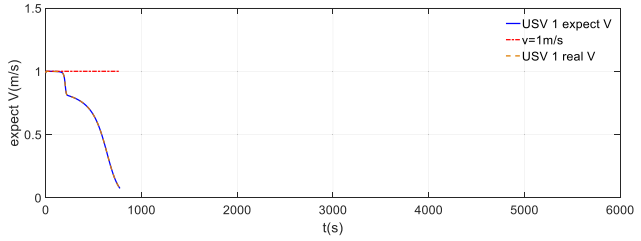

FIGURE 27. The speed contrast curve of USV no.1 determined by ANSB.

seen from Fig.20 and Fig.21, under the safe distance set in this experiment, the MUSVs formation can complete the task, however, in the absence of obstacle avoidance strategy, the voyage time of was more than 5000 s. According to Fig.21, with gain coefficients of $\lambda_c = 0.001$, $\lambda_f = 0.020$, and $\lambda_a = 0.025$, the planned maximum speed is only 3/4 of the actual maximum speed of Dolphin-I when the NSB method is used.

Fig.22 and Fig.23 show the results obtained by the ANSB method with the collision avoidance strategies.

Fig.22 presents the formation track of MUSVs under the ANSB method. The dotted black line in Fig.20 is the formation every 20 s, and the solid yellow line represents the track of USV no. 3. The first third of the track of USV no. 3 is a wavy line. This is because according to the logical priority collision avoidance strategy, USV no. 3 regards USVs no. 2 and no. 1 as barriers to keep safe distance from. In this test, because the distance between the USV no. 2 and USV no. 3 was less than the safe distance, USV no. 3 gave way. Moreover, because the minimum rotation radius of the Dolphin series USV is 8 m, sinusoidal motion is generated when two adjacent planning nodes are relatively close.

Fig. 23 shows a comparison curve between the actual speed and the expected speed determined by the ANSB method for USV no.1 as an example. It can be seen from the figure that the expected speed of the USV was always within the range of the maximum maneuvering speed (1 m/s) of the Dolphin series MUSVs, and it declined slowly. The motion control subsystem could well keep up with the change in expected speed, and the speed approaching the target point gradually approached 0.

In the second group of comparative tests, the safe distance between two USVs was set as 10 m. The test results of the two methods are shown in Fig. 24 to Fig. 27.

When the safe distance between the USVs was set at 10 m and the NSB method without a collision avoidance strategy was used, USVs no.1, no. 4, and no. 5 all performed obstacle avoidance behaviors, and the three vehicles interacted with each other, causing the USV no. 4 to deviate from the navigation path (Fig. 24). Furthermore, the planned speed of USV no. 1 for some time far exceeded the maneuverability of Dolphin-I (Fig. 25). Fig. 26 shows that with the ANSB method the MUSVs can still maintain the formation to complete the task. Fig.25 and Fig.27 show that utilizing the ANSB method can help MUSVs complete tasks more quickly.

V. CONCLUSION

1) By analyzing the NSB method theory and the USV dynamic model, we found that when the traditional NSB method is applied to the MUSVs formation control, problems

such as saturated planning and lengthy planning easily occur. The lack of operating conditions adaptability is not conducive to engineering applications.

2) We proposed a vector graph behavior determination method to determine the behavior priority from the perspective of the matrix theory. Compared with the traditional experiential behavior prioritization method, the vector graph behavior determination method is more rigorous, has higher controllability, and is convenient for parameter analysis and debugging.

3) The proposed redefined behavioral motion model makes the speed in each working condition adaptively and within the maneuverability range of the USV. Furthermore, the proposed logical priority collision avoidance strategy simplifies the process of obstacle avoidance and facilitates formation task efficiently. The simulation illustrates the effectiveness of the proposed ANSB control method.

For future work, this can be extended towards the formation control of heterogeneous MUSVs. This will help various USVs collaborate on tasks.

REFERENCES

[1] Y.-L. Liao, M.-J. Zhang, L. Wan, and Y. Li, "Trajectory tracking control for underactuated unmanned surface vehicles with dynamic uncertainties," *J. Central South Univ.*, vol. 23, no. 2, pp. 370–378, 2016.

[2] N. Mišković, Z. Vukić, M. Bibuli, G. Bruzzone, and M. Caccia, "Fast in-field identification of unmanned marine vehicles," *J. Field Robot.*, vol. 28, no. 1, pp. 101–120, 2011.

[3] L. Elkins, D. Sellers, and W. R. Monach, "The autonomous maritime navigation (AMN) project: Field tests, autonomous and cooperative behaviors, data fusion, sensors, and vehicles," *J. Field Robot.*, vol. 27, no. 6, pp. 790–818, 2010.

[4] S.-L. Dai, S. He, H. Lin, and C. Wang, "Platoon formation control with prescribed performance guarantees for USVs," *IEEE Trans. Ind. Electron.*, vol. 65, no. 5, pp. 4237–4246, May 2018. doi: 10.1109/TIE.2017.2758743.

[5] J.-X. Xi, C. Wang, H. Liu, and Z. Wang, "Dynamic output feedback guaranteed-cost synchronization for multiagent networks with given cost budgets," *IEEE Access*, vol. 6, pp. 28923–28935, 2018.

[6] J. Xi, C. Wang, H. Liu, and L. Wang, "Completely distributed guaranteed-performance consensualization for high-order multiagent systems with switching topologies," *IEEE Trans. Syst., Man, Cybern. Syst.*, vol. 49, no. 7, pp. 1338–1348, Jul. 2019.

[7] B. C. Shah, P. Švec, I. R. Bertaska, A. J. Sinisterra, W. Klinger, K. von Ellenrieder, M. Dhanak, and S. K. Gupta, "Resolution-adaptive risk-aware trajectory planning for surface vehicles operating in congested civilian traffic," *Auton. Robots*, vol. 40, no. 7, pp. 1139–1163, 2016.

[8] M. Bibuli, G. Bruzzone, M. Caccia, and A. Gasparri, "Swarm-based path-following for cooperative unmanned surface vehicles," *J. Eng. Maritime Environ.*, vol. 228, no. 2, pp. 192–207, 2014.

[9] Z. Peng, D. Wang, T. Li, and Z. Wu, "Leaderless and leader-follower cooperative control of multiple marine surface vehicles with unknown dynamics," *Nonlinear Dyn.*, vol. 74, nos. 1–2, pp. 95–106, 2013.

[10] L. Briñón-Arranz, A. Pascoal, and A. P. Aguiar, "Adaptive leader-follower formation control of autonomous marine vehicles," in *Proc. 53rd IEEE Conf. Decis. Control*, Dec. 2014, pp. 5328–5333.

[11] F. Arrichiello, S. Chiaverini, and T. I. Fossen, "Formation control of marine surface vessels using the null-space-based behavioral control," *Group Coordination Cooperat. Control*, vol. 336, pp. 1–19, Jul. 2006.

[12] X. M. Liang and X. Li, "A new decentralized planning strategy for flocking of swarm robots," *J. Comput.*, vol. 5, no. 6, pp. 914–921, 2010.

[13] G. Antonelli, F. Arrichiello, F. Caccavale, and A. Marino, "Decentralized centroid and formation control for multi-robot systems," in *Proc. IEEE Int. Conf. Robot. Automat.*, May 2013, pp. 3511–3516.

[14] L.-B. Wu, X.-K. Wang, H. Zhang, and Z.-Q. Zheng, "A null-space-based control method for soccer robots," *Comput. Eng. Sci.*, vol. 33, no. 9, pp. 145–150, 2011.

[15] H. Yao, Q. Zeng, and M. Hu, "Null-space-based coordinated control of spacecraft formation," in *Proc. 10th China Conf. Syst. Simul. Technol. Appl. (CCSSTA)*, 2009, vol. 448, no. 2, pp. 548–551.

[16] J. Chen, M. Gan, J. Huang, L. Dou, and H. Fang, "Formation control of multiple Euler-Lagrange systems via null-space-based behavioral control," *Sci. China Inf. Sci.*, vol. 59, no. 1, pp. 1–11, 2016.

[17] Q. Yang, H. Fang, Y. Mao, and J. Huang, "Distributed tracking for networked Euler-Lagrange systems without velocity measurements," *J. Syst. Eng. Electron.*, vol. 25, no. 4, pp. 671–680, Aug. 2014.

[18] Y.-L. Liao, Y.-M. Li, L.-F. Wang, Y. Li, and Q.-Q. Jiang, "Heading control method and experiments for an unmanned wave glider," *J. Central South Univ.*, vol. 24, no. 11, pp. 2504–2512, 2017.

[19] J. Ghommam and F. Mnif, "Coordinated path-following control for a group of underactuated surface vessels," *IEEE Trans. Ind. Electron.*, vol. 56, no. 10, pp. 3951–3963, Oct. 2009. doi: 10.1109/TIE.2009.2028362.

[20] H. Chen, L. Z. Li, and G. Z. Li, "Structure of the generalized zero space of matrix," *J. Inf. Eng. Univ.*, vol. 8, no. 1, pp. 47–48, and 48–109, 2007.

[21] F. Arrichiello, S. Chiaverini, and T. I. Fossen, "Formation control of underactuated surface vessels using the null-space-based behavioral control," in *Proc. IEEE/RSJ Int. Conf. Intell. Robots Syst.*, Oct. 2006, pp. 5942–5947.

[22] Y.-L. Liao, M.-J. Zhang, and L. Wan, "Serret-Frenet frame based on path following control for underactuated unmanned surface vehicles with dynamic uncertainties," *J. Central South Univ.*, vol. 22, no. 1, pp. 214–223, 2015.

[23] C. R. Sonnenburg and C. A. Woolsey, "Modeling, identification, and control of an unmanned surface vehicle," *J. Field Robot.*, vol. 30, no. 3, pp. 371–398, 2013.

[24] Y. Li, L. Wang, Y. Liao, Q. Jiang, and K. Pan, "Heading MFA control for unmanned surface vehicle with angular velocity guidance," *Appl. Ocean Res.*, vol. 80, pp. 57–65, Nov. 2018.

[25] G. Zhang, C. Huang, X. Zhang, and W. Zhang, "Practical constrained dynamic positioning control for uncertain ship through the minimal learning parameter technique," *IET Control Theory Appl.*, vol. 12, no. 18, pp. 2526–2533, 2018.

[26] G. Zhang, Y. Deng, W. Zhang, and C. Huang, "Novel DVS guidance and path-following control for underactuated ships in presence of multiple static and moving obstacles," *Ocean Eng.*, vol. 170, pp. 100–110, Dec. 2018.

[27] Y. Liao, Q. Jiang, T. Du, and W. Jiang, "Redefined output model-free adaptive control method and unmanned surface vehicle heading control," *IEEE J. Ocean. Eng.*, to be published. doi: 10.1109/JOE.2019.2896397.

[28] Y. Liao, Z. Jia, W. Zhang, Q. Jia, and Y. Li, "Layered berthing method and experiment of unmanned surface vehicle based on multiple constraints analysis," *Appl. Ocean Res.*, vol. 86, pp. 47–60, May 2019.

[29] J. Fan, Y. Li, Y. Liao, W. Jiang, L. Wang, Q. Jia, and H. Wu, "Second path planning for unmanned surface vehicle considering the constraint of motion performance," *J. Mar. Sci. Eng.*, vol. 7, no. 4, p. 104, 2019. doi: 10.3390/jmse7040104.

JIAJIA FAN received the B.Eng. degree in naval architecture and ocean engineering from Harbin Engineering University, Harbin, China, in 2015, where she is currently pursuing the Ph.D. degree. Her research interest includes formation control and motion control technologies of unmanned marine vehicles.

YULEI LIAO received the B.Eng. degree in naval architecture and ocean engineering and the Ph.D. degree in design and manufacture of marine structures from Harbin Engineering University, Harbin, China, in 2007 and 2012, respectively, where he is currently an Associate Professor with the College of Shipbuilding Engineering. His research interests include intelligent marine vehicles, USV swarming, ocean energy driving marine vehicles, new-concept marine vehicles, and intelligent motion control.

YE LI received the B.Eng. degree in naval architecture and ocean engineering and the M.S. and Ph.D. degrees in design and manufacture of marine structures from Harbin Engineering University, Harbin, China, in 2001, 2004, and 2007, respectively, where he is currently a Professor with the College of Shipbuilding Engineering. He is elected in the New Century Excellent Talents Supporting Project by the Ministry of Education and the National Special Support Program for High-level Talents. His research interests include intelligent marine vehicles, maneuverability, motion control, underwater navigation, and system simulation. He serves as an Associate Editor for the *Journal of Harbin Engineering University*.

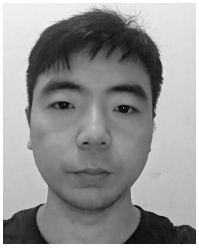

QUANQUAN JIANG received the B.Eng. degree in naval architecture and ocean engineering from HIT, Weihai, China, in 2015. He is currently pursuing the Ph.D. degree with Harbin Engineering University, Harbin, China. His research interests include intelligent marine vehicles and intelligent motion control.

LEIFENG WANG received the B.Eng. degree in naval architecture and ocean engineering from Harbin Engineering University, Harbin, China, in 2014, where he is currently pursuing the Ph.D. degree in design and manufacture of marine structures. His research interests include dynamics modeling and motion control technologies of unmanned marine vehicles.

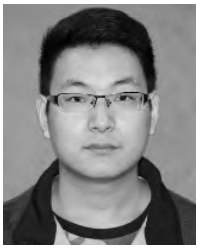

WEN JIANG received the B.Eng. degree in naval architecture and ocean engineering from the Wuhan University of Technology, Wuhan, China, in 2017. He is currently pursuing the M.Eng. degree in naval architecture and ocean engineering with the Science and Technology on Underwater Vehicle Laboratory, Harbin Engineering University, Harbin, China. He majors in ship and marine structure design and manufacturing. His research interests include USV motion control and cooperative control.